

# Origins of the Sensitivity of Molecular Vibrations to Electric Fields: Carbonyl and Nitrosyl Stretches in Model Compounds and Proteins

Eun Sun Park and Steven G. Boxer\*

Department of Chemistry, Stanford University, Stanford, California 94305-5080

Received: January 31, 2002; In Final Form: April 3, 2002

The vibrational Stark effect (VSE) is the effect of an electric field on the vibrational spectrum. Typically, the largest change induced by an electric field is the linear frequency shift whose sensitivity is known as the Stark tuning rate  $\Delta\mu$ ; the magnitude and direction of  $\Delta\mu$  are measured by VSE spectroscopy. This can be used to calibrate the sensitivity of vibrational frequencies to local electrostatic fields in proteins. To be most useful, it is critical to obtain a sensitive probe that has a large  $\Delta\mu$ , and understanding the origins of  $\Delta\mu$  is required. The Stark tuning rate arises from two distinct origins: mechanical anharmonicity ( $\Delta\mu_{\text{anh}}$ ) and the change of the bond force constant because of the electronic polarizability ( $\Delta\mu_{\text{bond}}$ ), with  $\Delta\mu = \Delta\mu_{\text{anh}} + \Delta\mu_{\text{bond}}$ . These two origins were quantitatively investigated for carbonyl and nitrosyl stretches in model compounds and proteins by IR and VSE spectroscopy. The contribution of  $\Delta\mu_{\text{anh}}$  was found to dominate  $\Delta\mu$  for carbonyl stretches in acetone, methyl vinyl ketone, and 1-methyl-2-pyrrolidinone despite their different degrees of electron delocalization. In contrast, the presence of  $d-\pi^*$  back-bonding when CO is bound to the heme causes  $\Delta\mu_{\text{bond}}$  to be more significant, giving rise to large variations in the Fe–CO and C–O stretch frequencies in heme protein variants such as myoglobin mutants, with a strong negative correlation between  $\bar{\nu}_{\text{Fe–CO}}$  and  $\bar{\nu}_{\text{C–O}}$ . The back-bonding also increases  $\Delta\mu_{\text{anh}}$  because of the enhanced effective charges on the CO oscillator. By comparison, the small variation in Fe–NO stretch frequency and the absence of a strong negative correlation between Fe–NO and N–O stretch frequencies for NO bound to the heme iron in myoglobin variants suggest that  $\Delta\mu_{\text{Fe–NO}}$  is much smaller than  $\Delta\mu_{\text{Fe–CO}}$ , possibly because of less back-bonding in heme–NO complexes. Nevertheless,  $\Delta\mu_{\text{N–O}}$  has approximately the same magnitude as  $\Delta\mu_{\text{C–O}}$  when bound to heme, suggesting that the anharmonic effect on VSE is larger for the N–O stretch than that for C–O stretch.

## Introduction

Electrostatic fields in condensed phase systems can profoundly affect the physical properties and reactivity of dissolved molecules. These effects can be especially important in ordered environments such as fabricated nanostructures or biological macromolecules. For example, local electrostatic fields play an essential role in proteins, including folding, molecular recognition, and catalytic functions.<sup>1–3</sup> Although a large body of computational data is available, it is difficult to directly measure and map the electrostatic field in proteins, and there have only been a few experimental measurements reported.<sup>4–11</sup>

An electric field, whether internal because of a solvent or externally applied, perturbs molecular vibrations. The changes induced by an applied external electric field can be measured by vibrational Stark effect (VSE) spectroscopy. Typically, the largest change in the IR spectrum induced by an electric field is a linear frequency shift, and the sensitivity of the shift is known as the Stark tuning rate,  $\Delta\mu$ , typically expressed in  $\text{cm}^{-1}/[\text{MV}/\text{cm}^{-1}]$  or in Debye. The frequency shift induced by local disorder in the electric field from the solvent is a major source of inhomogeneous broadening in condensed phase systems. In an organized system such as a protein, variations in the local electric field are often directed and larger than those from local disorder. This leads to observable vibrational band shifts in different locations in a protein, in different mutants, upon

protonation or deprotonation of nearby residues, or upon interaction with a ligand or another protein. If larger than inhomogeneous broadening, these vibrational band shifts can be used to probe the local electrostatic field if the sensitivity of the vibration to a field, i.e., the Stark tuning rate, is known. We have recently developed straightforward methods for measuring the vibrational Stark effect and applied them to simple molecules in condensed phase samples<sup>12,13</sup> and proteins.<sup>11,14</sup> Therefore, understanding the origins of the Stark tuning rate is important both for studying the physics of molecular vibrations and also for optimizing the utility of this approach to sensitively probe electrostatic fields in proteins.

The origins of the VSE have been studied extensively by theoretical approaches;<sup>15–19</sup> however, there have been only a few quantitative experimental analyses.<sup>13,20</sup> The VSE arises from the change of dipole moment associated with a vibrational transition as hinted from the notation of  $\Delta\mu$  for the Stark tuning rate. The Stark tuning rate has two distinct origins:<sup>19</sup> the bond anharmonicity ( $\Delta\mu_{\text{anh}}$ ) and the field-dependent bond constant that is due to the electronic polarizability ( $\Delta\mu_{\text{bond}}$ ). These are illustrated schematically in Figure 1. We obtain  $\Delta\mu$  from VSE spectroscopy, and it should be the sum of  $\Delta\mu_{\text{anh}}$  and  $\Delta\mu_{\text{bond}}$ :

$$h\Delta\nu = -\Delta\mu \cdot F = -(\Delta\mu_{\text{anh}} + \Delta\mu_{\text{bond}}) \cdot F \quad (1)$$

where  $h$  is Planck's constant,  $\nu$  is the light frequency, and  $F$  is the electric field felt by the chromophore.<sup>21</sup> The notation  $\Delta\mu$  is, however, somewhat misleading as the Stark tuning rate is not exactly equivalent to the difference in dipole moments

\* To whom correspondence should be addressed. Phone: (650)723-4482. Fax: (650)723-4817. E-mail: Sboxer@stanford.edu.

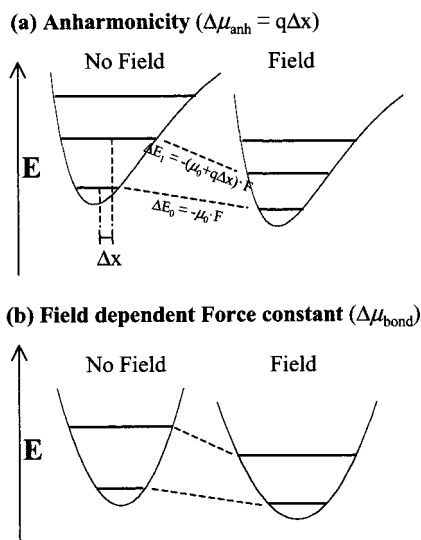


**Figure 1.** Schematic illustration of the effect of an electric field on a vibrational transition energy leading to the observed Stark tuning rate  $\Delta\mu$ . (a) Mechanical anharmonicity leads to a displacement ( $\Delta x$ ) in the average position of the oscillator between the lowest and first excited vibrational levels, leading to a change in dipole moment  $\Delta\mu_{\text{anh}}$ .  $q$  is the effective charge of the oscillator. (b) A change of the bond force constant in an applied electric field because of electronic polarizability leads to a contribution to the Stark tuning rate denoted  $\Delta\mu_{\text{bond}}$ . The overall Stark tuning rate observed in a VSE measurement is  $\Delta\mu = \Delta\mu_{\text{anh}} + \Delta\mu_{\text{bond}}$ .

between the ground and excited vibrational levels at a high level of theory.<sup>16</sup> This discrepancy can be ignored at the level of the analysis used here though.

In a simple model,  $\Delta\mu_{\text{anh}}$  can be represented by a displacement of the effective charge  $q$  by a distance  $\Delta x$  which is due to the mechanical anharmonicity of the potential surface as shown in Figure 1a.<sup>22</sup> The anharmonicity constant  $x_e$  is defined as the difference in transition energy (in  $\text{cm}^{-1}$ ) between the 0–1 and 1–2 transitions divided by  $2\bar{\nu}_e$ ,  $(\bar{\nu}_{0-1} - \bar{\nu}_{1-2})/2\bar{\nu}_e$ , where  $\bar{\nu}_e$  is the oscillator frequency when the harmonic approximation is applied. The values of  $(\bar{\nu}_{0-1} - \bar{\nu}_{1-2})$  for various oscillators have been reported from several different experiments and/or calculations and are available in the literature. The magnitude of the transition moment of an oscillator  $|M|$  is obtained in units of Debye (D) from the IR intensity of the band and gives the effective charge  $q$ :<sup>22</sup>

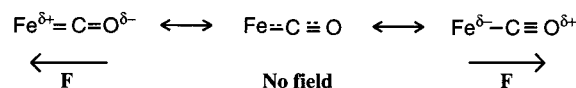
$$|M| = \sqrt{\frac{3\epsilon_0 hc \ln 10}{2\pi^2 N_A \bar{\nu}}} \int \epsilon(\bar{\nu}) d\bar{\nu} = \frac{q}{2\pi} \sqrt{\frac{h}{2cm\bar{\nu}}} \quad (2)$$

where  $\epsilon_0$  is the electrical permittivity of vacuum,  $h$  is Planck's constant,  $\bar{\nu}$  is the light frequency in wavenumbers,  $N_A$  is Avogadro's number,  $\epsilon(\bar{\nu})$  is the extinction coefficient,  $c$  is the speed of light, and  $m$  is the reduced mass. When  $|M|$  and  $x_e$  are combined,  $|\Delta\mu_{\text{anh}}|$  is obtained:

$$|\Delta\mu_{\text{anh}}| = q\Delta x = 3q\sqrt{\frac{\hbar\omega x_e}{2k_2}} = 3|M|\sqrt{x_e} \quad (3)$$

Figure 1b shows the contribution of  $\Delta\mu_{\text{bond}}$  to the vibrational Stark effect. The harmonic force constant can be varied by an electric field because of the electronic polarizability. For example, a particular resonance structure can be relatively more stabilized in the presence of an electric field, giving rise to the change in the dipole moment and the bond force constant. The change of the bond force constant in the presence of an electric

### SCHEME 1



field yields the change of the transition energy between vibrational levels and thus the Stark effect. The magnitude of  $\Delta\mu_{\text{bond}}$  is obtained by the perturbation theory:<sup>16–19</sup>

$$|\Delta\mu_{\text{bond}}| = \frac{\hbar\omega|v_2'|}{k_2} \quad (4)$$

where  $v_2'$  expresses the sensitivity of the force constant to an electric field and is referred as dipole nonlinearity in ref 17. More details on the definition of  $v_2'$  are available in ref 19.

We recently reported a quantitative measurement of the Stark tuning rate for CO bound to the heme iron in model porphyrins and in myoglobin (Mb).<sup>11</sup> Interestingly, the Stark tuning rate of CO bound to the heme ( $\sim 0.14 \text{ D/f}$  or  $2.4/\text{f cm}^{-1}/[\text{MV/cm}^{-1}]$ , where  $f$  is the local field correction factor<sup>21</sup>) was observed to be much larger than for free CO dissolved in an organic solvent ( $\sim 0.04 \text{ D/f}$ ). The higher sensitivity of  $\bar{\nu}_{\text{CO}}$  to an electric field when it is bound to heme could be anticipated given the large variations in  $\bar{\nu}_{\text{CO}}$  shifts that is observed when mutations expected to affect the electrostatic field are introduced near the bound CO in Mb.<sup>23,24</sup> This observation has been made more quantitative by correlating calculated electrostatic potentials for various Mb mutants and their CO stretch frequencies,<sup>25</sup> with the slope of the correlation given by  $|\Delta\mu|$ .<sup>11</sup> In addition to bond anharmonicity, the large sensitivity of  $\bar{\nu}_{\text{CO}}$  for CO bound to heme may be related to  $\pi$  back-bonding between CO and Fe. Upon application of an electric field, different resonance structures of the Fe-bound CO may be differentially stabilized, for example (see Scheme 1),<sup>11,23,25</sup> and this may enhance  $\Delta\mu_{\text{bond}}$ .

To better understand the origins of the Stark effect, we undertook a more systematic and quantitative investigation of simple model compounds. A set of organic compounds that have a carbonyl group and are expected to have force constants with different sensitivities to an electric field (acetone, methyl vinyl ketone (MVK), and 1-methyl-2-pyrrolidinone (NMP)) was selected. In the following, we report quantitative measurements of  $\Delta\mu$  and  $\Delta\mu_{\text{anh}}$  for this set of organic compounds and compare them with those for CO bound to the heme and free CO. The difference is used to explain the well-documented empirical correlation between Fe–CO stretch and C–O stretch frequencies for the CO-bound heme complexes.<sup>26</sup> Related to these results, the absence of a correlation between Fe–NO and N–O stretch frequencies for NO bound to Mb mutants is also investigated and rationalized.

### Experimental Section

#### IR Absorption and VSE for Carbonyl Compounds.

Anhydrous acetone (99.9%), methyl vinyl ketone (MVK, 99%), 1-methyl-2-pyrrolidinone (NMP, 99.5%), and 2-methyl tetrahydrofuran (2MeTHF, 99%) were purchased from Aldrich and used without further purification. The samples were dissolved in a glass-forming solvent, 2MeTHF, for the measurements. Sample concentrations ranged from 100 mM to 300 mM, but no concentration dependent effects were observed in this range for both the IR intensity and the vibrational Stark effect.

VSE spectra were obtained on a Bruker IFS 66V/S FTIR spectrometer with a nitrogen-cooled MCT detector at  $0.5 \text{ cm}^{-1}$  resolution. Samples were loaded into an IR Stark cell consisting of a pair of nickel-coated ( $\sim 50 \text{ \AA}$  thick) calcium fluoride

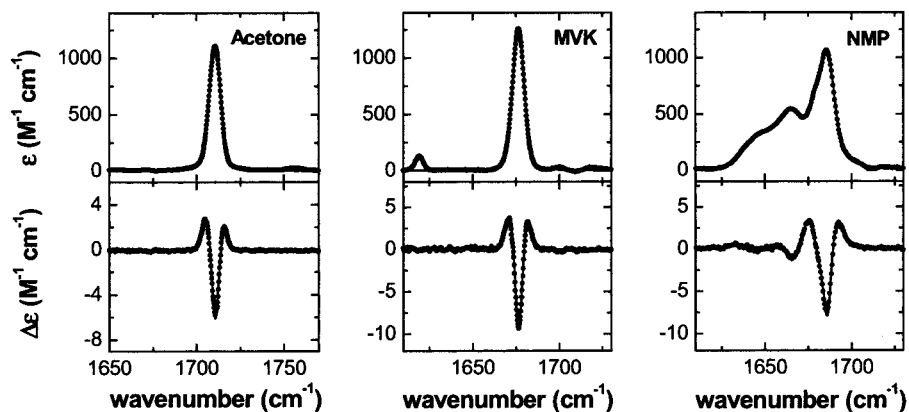


**Figure 2.** IR absorption spectra (top panels; solvent subtracted) and vibrational Stark spectra (bottom panels, dotted curve) for acetone, MVK, and NMP in 2MeTHF. The spectra were taken at 77 K and in normal incidence ( $\chi = 0^\circ$ ). The solid lines in the absorption and Stark panels are the best fits. The Stark spectra are scaled to 1 MV/cm applied electric field to facilitate comparison.

windows separated by 30  $\mu\text{m}$  Teflon spacers. The nickel coating acts as a semitransparent (50–80% transparent in the region of interest) electrode for the application of an electric field across the sample for VSE measurements. The cell containing the sample was immersed in a liquid  $\text{N}_2$  immersion cryostat operating at  $\sim 77$  K.<sup>27</sup> Both absorption and VSE spectra were taken with the same sample simultaneously. A single scan was obtained with the field off, then a scan with the field on (typically about +2 kV), then another scan with the field off, and finally a scan with the same magnitude of the field on, but in the opposite direction. This cycle was repeated at least 512 times for each Stark spectrum that is the average of the field-on scans minus the average of the field-off scans (see ref 13 for further details). At least three such VSE measurements were performed for each sample with different applied potentials (1.0–2.5 kV, corresponding to an applied field of 0.5–1 MV/cm). The absorption spectrum was directly obtained from the average of the field-off scans subtracted by a solvent spectrum.

As described in detail elsewhere, the Stark spectrum of an immobilized, isotropic sample can be described as the sum of the derivatives of the absorption spectrum:<sup>13</sup>

$$\Delta A(\bar{\nu}) = (F_{\text{ext}}f)^2 \left\{ A_\chi A(\bar{\nu}) + \frac{B_\chi}{15hc} \bar{\nu} \frac{d}{d\bar{\nu}} \left( \frac{A(\bar{\nu})}{\bar{\nu}} \right) + \frac{C_\chi}{30h^2c^2} \bar{\nu} \frac{d^2}{d\bar{\nu}^2} \left( \frac{A(\bar{\nu})}{\bar{\nu}} \right) \right\} \quad (5)$$

where  $F_{\text{ext}}$  is the external applied field,  $f$  is the local field correction,<sup>21</sup>  $h$  is Planck's constant, and  $c$  is the speed of light. The coefficients  $A_\chi$ ,  $B_\chi$ , and  $C_\chi$  are associated with molecular properties of the system.<sup>13</sup>  $C_\chi$  depends only on  $\Delta\mu$  and  $\zeta$ , the angle between  $\Delta\mu$  and the transition moment direction, and is given by

$$C_\chi = |\Delta\mu|^2 [5 + (3 \cos^2 \chi - 1)(3 \cos^2 \zeta - 1)] \quad (6)$$

$\zeta$  is determined from the ratio of the Stark spectra taken at different experimental angles  $\chi$  between the direction of polarized light and the applied field direction. The coefficients in eq 5 are obtained by fitting the numerical derivatives of the absorption spectrum to the Stark spectrum.<sup>13</sup>

**IR Absorption Spectroscopy of CO Bound to MbCO and Photolyzed CO.** Wild-type human Mb<sup>28</sup> was expressed and purified from *Escherichia coli* as described elsewhere.<sup>29</sup> Protein solutions were concentrated to  $\sim 7$  mM in 50/50 glycerol/buffer (100 mM phosphate buffer, pH 7). The MbCO samples were

prepared as described elsewhere.<sup>29</sup> The UV/vis absorption spectrum was taken to confirm the formation of the MbCO complex and to determine the exact concentration of the protein solution ( $\epsilon_{543} = 14.5$  OD/mM cm;  $\epsilon_{597} = 13$  OD/mM cm).<sup>30</sup>

The low-temperature FTIR spectra were obtained on the same spectrometer with 2  $\text{cm}^{-1}$  resolution and an InSb detector. The sample was loaded into an IR cell made with calcium fluoride windows and  $\sim 30$   $\mu\text{m}$  Teflon spacers, attached to the coldfinger of a continuous-flow liquid helium cryostat (Janis) and then cooled to 5 K. Spectra were taken at 5 K before and after photolysis of bound CO using a 300 W halogen lamp to obtain spectra of CO bound to Mb and photolyzed CO, respectively. The photolysis yield for MbCO is almost 1, and rebinding does not occur at 5 K.<sup>31,32</sup>

## Results

**IR Absorption and Vibrational Stark Spectroscopy of Carbonyl Compounds.** The IR absorption and vibrational Stark spectra of the carbonyl stretch in acetone, MVK, and NMP are shown in the top and bottom panels, respectively, of Figure 2. The samples were dissolved in 2MeTHF. Each compound shows an intense band in the absorption spectrum between 1625 and 1750  $\text{cm}^{-1}$  associated with a carbonyl stretch. MVK and NMP have lower C–O stretch frequencies than acetone (about 35  $\text{cm}^{-1}$  lower) because of the conjugation with the C=C double bond and the resonance contribution of electrons on the N atom that increases the single bond character of the CO bond, respectively. Both the conjugation and the resonance contribution weaken the CO bond strength and lower the C–O stretch frequency. The Stark spectra are shown in the bottom panels (dotted curves), and their fits are overlaid on the data. The Stark spectra for acetone and MVK are very similar to the second derivatives of their absorption spectra. The  $|\Delta\mu|$  values were obtained from the second derivative contribution to the Stark spectrum using eqs 5 and 6.<sup>33</sup> In the case of NMP, multiple peaks were observed, possibly from different conformations of the molecule. The absorption and the Stark spectra were simultaneously fit with four modified Voigt bands and their derivatives, respectively.<sup>13</sup> The fits are overlaid on the data and shown in Figure 2. It is observed that the Stark spectrum is very close to the second derivative of its absorption spectrum giving approximately the same  $|\Delta\mu|$  across most of the band: 0.070, 0.071, and 0.063 D/f for the bands at 1646, 1665, and 1686  $\text{cm}^{-1}$ , respectively. The minor band at 1679  $\text{cm}^{-1}$  (less than 15% of the total intensity) has a much smaller  $|\Delta\mu|$  (0.044 D/f); it may not be associated with the C–O stretch or may be



**TABLE 1: IR Absorption and Vibrational Stark Effect Data for the CO Stretch<sup>a</sup>**

	acetone <sup>b</sup>	MVK <sup>b</sup>	NMP <sup>b</sup>	MbCO <sup>b</sup>	CO <sup>b</sup>
$\bar{\nu}$ (cm <sup>-1</sup> ) <sup>c</sup>	1711	1676	1685	1945	2130
$B$ (KM/mol)	97	109	281	313	14 <sup>d</sup>
$ M $ (D)	0.23	0.24	0.39	0.38	0.077
$\bar{\nu}_{0-1} - \bar{\nu}_{1-2}$ (cm <sup>-1</sup> ) <sup>e,f</sup>	16	16	16	26	27
$ \Delta\mu_{\text{anh}} $ (D)	0.047	0.051	0.081	0.094	0.019
$ \Delta\mu $ (D/f)	0.045	0.049	0.068 <sup>g</sup>	0.14	0.04

<sup>a</sup> All spectra were taken at 77 K. <sup>b</sup> Acetone, MVK, NMP, and CO were dissolved in 2MeTHF. MbCO was dissolved in 50% glycerol/phosphate buffer (pH 7). <sup>c</sup> Peak maximum. <sup>d</sup> The IR intensity was obtained from the photolysis experiment of MbCO. See text and Figure 3 for details. <sup>e</sup> Data taken from refs 35 and 36 for acetone and assumed to be the same for MVK. For NMP, the value observed for *N,N*-dimethylacetamide in ref 37 was used. The values were taken from refs 38 and 39 for MbCO and ref 40 for CO. <sup>f</sup> See ref 34. <sup>g</sup> Average  $|\Delta\mu|$ . See the text.

a Fermi resonant mode. Theory predicts that  $|\Delta\mu|$  of a resonant mode is a linear combination of  $|\Delta\mu|$  of the uncoupled modes.<sup>19</sup> If the band at 1679 cm<sup>-1</sup> is a Fermi resonant mode between the C–O stretch mode and another mode with a small  $|\Delta\mu|$ , the  $|\Delta\mu|$  of a resonant mode would be much smaller than that of C–O stretch. Similar results were obtained when NMP was dissolved in different solvents such as methyl cyclohexane or perdeuterated methyl cyclohexane (data not shown). This suggests that this minor band might originate from either a vibrational mode in NMP that is not associated with a C–O stretch or a Fermi resonance occurring with a mode in NMP. Peak maxima ( $\bar{\nu}$ ) and IR intensities ( $B$ ) from IR absorption measurements,  $|\Delta\mu|$ 's from VSE measurements, and calculated transition moments ( $|M|$ ) and  $|\Delta\mu_{\text{anh}}|$ 's using eqs 2 and 3, respectively, are listed in Table 1. The differences in transition energy between the 0–1 and 1–2 transitions ( $\bar{\nu}_{0-1} - \bar{\nu}_{1-2}$ ) in Table 1 were taken from the literature.<sup>34–40</sup> It is observed that the  $|\Delta\mu|$ 's for these carbonyl stretches are approximately the same as  $|\Delta\mu_{\text{anh}}|$ 's obtained from the magnitude of the transition moment and the anharmonicity constants within the experimental error. (Experimental errors are less than 5% for both  $|\Delta\mu_{\text{anh}}|$  and  $|\Delta\mu|$ .) It is possible that the IR intensity,  $|M|$ , and  $|\Delta\mu_{\text{anh}}|$  for the C–O stretch in NMP might be somewhat overestimated from an overlap with a mode that is not associated with the C–O stretch or a Fermi resonance.

**IR Absorption and Vibrational Stark Spectroscopy of CO bound to Mb and Free CO in Frozen Glass.** The absorption spectra of the C–O stretch for CO bound to Mb (sometimes called A state CO) and photolyzed CO (sometimes called B state CO) are shown in Figure 3. When CO is photolyzed from a MbCO complex at 5 K, it is trapped in the protein and does not recombine.<sup>31,32</sup> The physical properties of photolyzed CO should be very similar to those of free CO in frozen glass because it is not covalently bound to the heme iron, and the IR frequency of photolyzed CO (2135 cm<sup>-1</sup>) is very close to that of CO dissolved in frozen 2MeTHF (2131 cm<sup>-1</sup>). Because it is difficult to accurately obtain the IR intensity<sup>41</sup> and thus the transition moment directly from free CO dissolved in 2MeTHF, a known concentration of MbCO complex was completely photolyzed, and a spectrum of the photolyzed CO was used to obtain the IR intensity of free CO. The vibrational Stark spectrum of CO bound to Mb was reported earlier and is presented again in Figure 4, along with the VSE spectrum of free CO in 2MeTHF. As reported earlier, the Stark spectra are very similar to the second derivatives of the absorption spectrum, and the Stark effect for free CO is significantly smaller than that for CO bound to Mb.<sup>11</sup> The experimental error for free CO

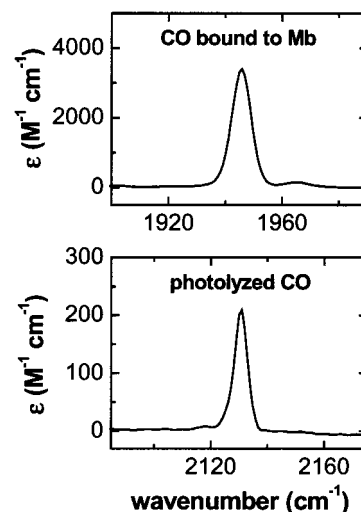


**Figure 3.** Photolysis difference absorption spectra of wild-type MbCO at 5 K in 50% glycerol/phosphate buffer at pH = 7. The top panel is the difference spectrum of unphotolyzed minus photolyzed in the 1900–1990 cm<sup>-1</sup> region showing the spectrum of CO bound to Mb, and the bottom panel is the difference spectrum of photolyzed minus unphotolyzed in the 1885–2175 cm<sup>-1</sup> region showing the spectrum of photolyzed CO trapped in the protein matrix. The latter was used to obtain the extinction coefficient of free CO as the concentration of the precursor MbCO is known accurately and the photolysis is complete and irreversible.

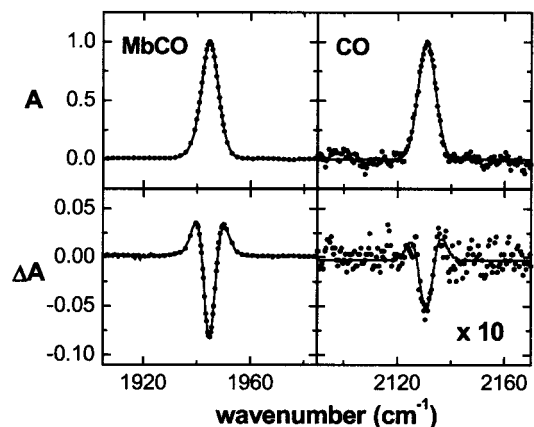


**Figure 4.** IR absorption spectra (top panels, dotted curve) and vibrational Stark spectra (bottom panels, dotted curve) for CO bound to wild-type Mb (left panels) and CO dissolved in 2MeTHF (right panels). The spectra were taken at 74 K and in normal incidence ( $\chi = 0^\circ$ ). The solid lines in the absorption and Stark spectra are the best fits. The absorption spectra are scaled to  $A = 1$ , and the Stark spectra are scaled to 1 MV/cm applied electric field to facilitate comparison. The actual absorbances are approximately  $\sim 0.1$  and  $\sim 0.003$ , respectively. (Spectra for MbCO were taken from ref 11.)

is considerably larger because of its smaller Stark effect and other experimental difficulties.<sup>41</sup> The results for CO bound to Mb and free CO are summarized in Table 1.

## Discussion

**Origins of Vibrational Stark Effects for Carbonyl Stretches.** As seen in Figure 2, MVK and NMP show much lower C–O stretch frequencies than acetone because of electron delocalization. One may predict that more electron delocalization in MVK and NMP would give higher field-dependence for the force constant of the C=O oscillator ( $\Delta\mu_{\text{bond}}$ ) than that of acetone. However, surprisingly, it is observed that the values of  $|\Delta\mu|$  are very close to  $|\Delta\mu_{\text{anh}}|$ , indicating that the contribution

of  $\Delta\mu_{\text{bond}}$  to  $\Delta\mu$  is almost negligible in all three compounds.<sup>42</sup> Neither the conjugation nor the resonance has a measurable effect on the sensitivity of the force constant to an electric field even though they cause more electron delocalization, weakening the C–O bond and lowering the C–O stretch frequency significantly. The slightly larger and much larger values of  $|\Delta\mu|$  observed for MVK and NMP, respectively, compared to that of acetone are, therefore, not due to the increased  $|\Delta\mu_{\text{bond}}|$  but are due to the enhancement of  $|\Delta\mu_{\text{anh}}|$  as the conjugation or the resonance gives larger effective charges on the CO oscillator. The larger effective charges also increase  $|M|$  and result in a stronger IR band.

As described earlier, it was previously speculated that the force constant of the C–O oscillator might be very susceptible to an electric field in the presence of  $d-\pi^*$  back-bonding between CO and Fe and that the strong field-dependence of the C–O force constant might be responsible for the large sensitivity of  $\bar{\nu}_{\text{C-O}}$  to an electric field observed for CO bound to heme.<sup>11,25</sup> For the quantitative analysis,  $|\Delta\mu|$  and  $|\Delta\mu_{\text{anh}}|$  were compared for the wild-type MbCO complex and free CO in frozen 2MeTHF. Unlike acetone, MVK, and NMP, the values of  $|\Delta\mu_{\text{anh}}|$  are much smaller than those of  $|\Delta\mu|$  for both CO bound to heme and free CO, which indicates that both  $\Delta\mu_{\text{anh}}$  and  $\Delta\mu_{\text{bond}}$  make significant contributions to  $|\Delta\mu|$ . The larger values of  $|\Delta\mu_{\text{bond}}|$  for CO bound to heme and free CO suggest that the force constant of the CO oscillator is more susceptible to a change of electric field when the CO bond has more triple than double bond character. A related result was obtained for the CN triple bond stretch in both aliphatic and aromatic nitriles, where  $|\Delta\mu_{\text{bond}}|$  is approximately 50% of  $|\Delta\mu|$ .<sup>13</sup> Ab initio calculation on a free CO gas molecule predicted that the contribution of  $|\Delta\mu_{\text{bond}}|$  is only 1–2% of  $|\Delta\mu|$  and negligible.<sup>18</sup> The mechanical anharmonic contribution  $|\Delta\mu_{\text{anh}}|$  for free CO in gas phase ( $\sim 0.026$  D) was predicted to be comparable to that in frozen glass (0.019 D).<sup>18</sup> The larger  $|\Delta\mu_{\text{bond}}|$  observed for free CO in frozen 2MeTHF compared to the value that was predicted for a free CO gas molecule by ab initio calculation may be due to the interaction between CO and solvent molecules which may stabilize the dipole moment change to an external electric field. It would be interesting to study the solvent effect on the relative contributions of  $\Delta\mu_{\text{anh}}$  and  $\Delta\mu_{\text{bond}}$ . This would be a difficult experiment as only a small number of solvents form a good glass and the VSE for CO itself is very small.

It is also observed that both  $|\Delta\mu_{\text{anh}}|$  and  $|\Delta\mu_{\text{bond}}|$  increase significantly when CO binds to the heme:  $\sim 0.075$  D increase for  $|\Delta\mu_{\text{anh}}|$  and  $\sim 0.025$  D increase for  $|\Delta\mu_{\text{bond}}|$ .<sup>43</sup> This result agrees with the previous speculation that  $|\Delta\mu_{\text{bond}}|$  of the CO oscillator becomes more susceptible to a change of electric field in the presence of back-bonding. However, the increase in  $|\Delta\mu_{\text{bond}}|$  is only  $\sim 25\%$  of the total increase in  $|\Delta\mu|$ , and the enhancement of  $|\Delta\mu_{\text{anh}}|$  is the main factor that leads to the larger Stark tuning rate when CO binds to Fe. As in the case of carbonyl compounds, the anharmonicity values are very similar for both free CO and heme-bound CO, and the increased  $|\Delta\mu_{\text{anh}}|$  for heme-bound CO can be explained to be mostly from the increased effective charge on the CO which is reflected by the enhanced IR intensity. In summary, the presence of back-bonding in CO bound to heme increases the sensitivity of the CO stretch to an electric field *both* by increasing the effective charge on the CO and thus  $|\Delta\mu_{\text{anh}}|$  and also by increasing the field-dependence of the bond force constant.

**Correlations between X–O Stretch and Fe–XO Stretch Frequencies in XO–heme Complexes (X = C or N).** Figures 5 and 6 show plots of the experimentally observed  $\bar{\nu}_{\text{X-O}}$  versus

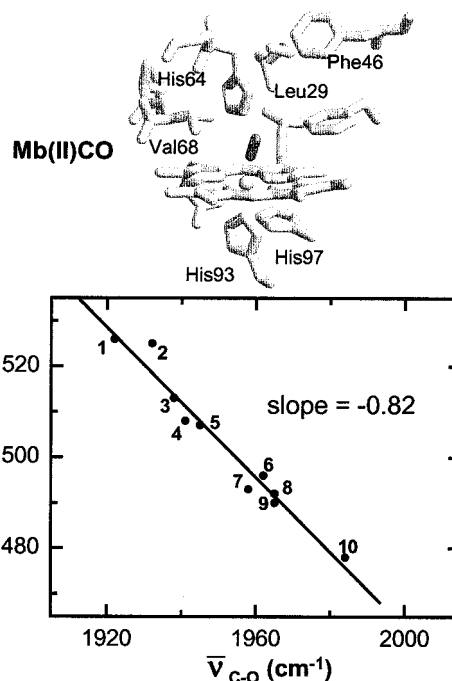


**Figure 5.** Plot of observed Fe–CO stretch and C–O stretch frequencies for CO bound to Mb variants (circles). The data are taken from ref 25. (1) V68N ( $\bar{\nu}_{\text{Fe-CO}} = 526$ ,  $\bar{\nu}_{\text{C-O}} = 1922$ ); (2) L29F ( $\bar{\nu}_{\text{Fe-CO}} = 525$ ,  $\bar{\nu}_{\text{C-O}} = 1932$ ); (3) H64Q/L29F ( $\bar{\nu}_{\text{Fe-CO}} = 513$ ,  $\bar{\nu}_{\text{C-O}} = 1938$ ); (4) wild-type ( $\bar{\nu}_{\text{Fe-CO}} = 508$ ,  $\bar{\nu}_{\text{C-O}} = 1941$ ); (5) H64Q ( $\bar{\nu}_{\text{Fe-CO}} = 507$ ,  $\bar{\nu}_{\text{C-O}} = 1945$ ); (6) F46V ( $\bar{\nu}_{\text{Fe-CO}} = 496$ ,  $\bar{\nu}_{\text{C-O}} = 1962$ ); (7) V68T ( $\bar{\nu}_{\text{Fe-CO}} = 493$ ,  $\bar{\nu}_{\text{C-O}} = 1958$ ); (8) H64G ( $\bar{\nu}_{\text{Fe-CO}} = 492$ ,  $\bar{\nu}_{\text{C-O}} = 1965$ ); (9) H64L ( $\bar{\nu}_{\text{Fe-CO}} = 490$ ,  $\bar{\nu}_{\text{C-O}} = 1965$ ); (10) H64V/V68T ( $\bar{\nu}_{\text{Fe-CO}} = 478$ ,  $\bar{\nu}_{\text{C-O}} = 1984$ ). The solid line is the best linear fit of circles.

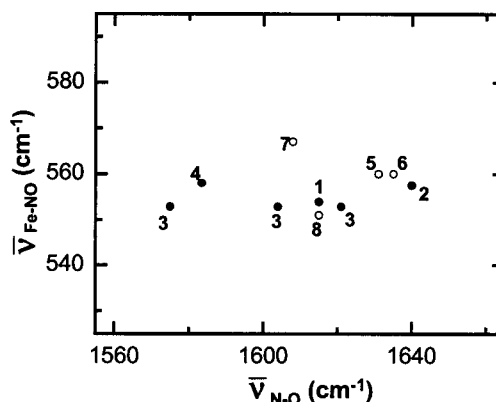


**Figure 6.** Plot of observed Fe–NO stretch and N–O stretch frequencies for NO bound to Mb variants. The data are taken from refs 44 and 45 for solid circles and open circles, respectively. The Fe–N stretch frequencies of open circles are taken from the peak maxima in the isotope difference spectra and not corrected for the actual frequencies.<sup>51</sup> (1) WT ( $\bar{\nu}_{\text{Fe-NO}} = 554$ ,  $\bar{\nu}_{\text{N-O}} = 1615$ ); (2) H64V ( $\bar{\nu}_{\text{Fe-NO}} = 557.5$ ,  $\bar{\nu}_{\text{N-O}} = 1640$ ); (3) V68L ( $\bar{\nu}_{\text{Fe-NO}} = 553$ ,  $\bar{\nu}_{\text{N-O}} = 1575, 1604, 1621$ ); (4) V68N ( $\bar{\nu}_{\text{Fe-NO}} = 558$ ,  $\bar{\nu}_{\text{N-O}} = 1583.5^{14}$ ); (5) H64G ( $\bar{\nu}_{\text{Fe-NO}} = 560$ ,  $\bar{\nu}_{\text{N-O}} = 1631$ ); (6) H64L ( $\bar{\nu}_{\text{Fe-NO}} = 560$ ,  $\bar{\nu}_{\text{N-O}} = 1635$ ); (7) L29W ( $\bar{\nu}_{\text{Fe-NO}} = 567$ ,  $\bar{\nu}_{\text{N-O}} = 1608$ ); (8) H64G ( $\bar{\nu}_{\text{Fe-NO}} = 551$ ,  $\bar{\nu}_{\text{N-O}} = 1615$ ).

$\bar{\nu}_{\text{Fe-XO}}$  for CO and NO bound to Mb variants, respectively.<sup>14,25,44,45</sup> As reported earlier, there is a strong negative linear correlation with a slope of  $-0.82$  between  $\bar{\nu}_{\text{C-O}}$  and  $\bar{\nu}_{\text{Fe-CO}}$  for MbCO complexes. However, in the case of MbNO variants, the variation of  $\bar{\nu}_{\text{Fe-NO}}$  is much smaller (the slope of the best linear fit is almost zero) than that of  $\bar{\nu}_{\text{Fe-CO}}$ , even though the variation of  $\bar{\nu}_{\text{N-O}}$  is as large as that of  $\bar{\nu}_{\text{C-O}}$  because  $\Delta\mu_{\text{C-O}} \approx \Delta\mu_{\text{N-O}}$ . The electrostatic fields sensed by the Fe–XO unit are affected by mutations introduced near the heme for the Mb

variants in Figures 5 and 6, and the Fe–XO and X–O stretches are accordingly shifted by an internal Stark effect.<sup>46</sup> The slope of the correlation can be represented as

$$\text{slope} = \frac{\Delta\bar{\nu}_{\text{Fe-XO}}}{\Delta\bar{\nu}_{\text{X-O}}} = \frac{\Delta\mu_{\text{Fe-XO}} \cdot F_{\text{protein}}}{\Delta\mu_{\text{X-O}} \cdot F_{\text{protein}}} = \frac{(\Delta\mu_{\text{anh,Fe-XO}} + \Delta\mu_{\text{bond,Fe-XO}}) \cdot F_{\text{protein}}}{(\Delta\mu_{\text{anh,X-O}} + \Delta\mu_{\text{bond,X-O}}) \cdot F_{\text{protein}}} \quad (7)$$

Given the linear geometry of Fe–C–O,<sup>47</sup> the angle between  $\Delta\mu$  and the electric field,  $F_{\text{protein}}$ , should be approximately the same for the Fe–CO and C–O stretches, and the slope of the correlation is the ratio of  $\Delta\mu_{\text{Fe-CO}}/\Delta\mu_{\text{C-O}}$ . From the magnitude of the slope and the measured  $\Delta\mu_{\text{C-O}}$  (see Table 1),  $\Delta\mu_{\text{Fe-CO}}$  is estimated to be 0.11 D/f.<sup>48</sup>

The geometry of Fe–NO is not as certain as that of Fe–CO because of the lack of a high-resolution crystal structure, and therefore,  $\Delta\mu_{\text{Fe-NO}}$  cannot be directly estimated from eq 7. However, the observed small variation of  $\bar{\nu}_{\text{Fe-NO}}$  in Mb variants obtained by resonance Raman spectroscopy clearly suggests that  $\Delta\mu_{\text{Fe-NO}}$  must be much smaller than  $\Delta\mu_{\text{Fe-CO}}$ . We have already shown that the presence of back-bonding in CO bound heme increases  $\Delta\mu_{\text{bond, C-O}}$  significantly. As shown in Scheme 1, the change of the force constant of the C–O stretch in an electric field is directly connected to the change of the force constant of the Fe–CO stretch. Therefore, we can easily imagine that  $\Delta\mu_{\text{bond}}$  for the Fe–CO stretch would also be large as was the case for the C–O stretch and result in the high sensitivity of the Fe–CO stretch frequency to an electric field ( $\Delta\mu_{\text{Fe-CO}} \approx 0.11$  D/f). This leads to the strong negative correlation between Fe–CO and C–O stretches. On the other hand, it has been suggested that the degree of back-bonding in the MbNO complex is smaller based on molecular orbital theory;<sup>49,50</sup> although CO has an empty  $\pi^*$  orbital, NO has one electron in a  $\pi^*$  orbital leading to a bent geometry and less  $d_{\pi}\pi^*$  back-bonding. A lesser degree of back-bonding in heme–NO complexes would lead to the smaller  $\Delta\mu_{\text{bond}}$  for the Fe–NO and N–O stretches and possibly lead to the smaller  $\Delta\mu_{\text{Fe-NO}}$ : unless  $\Delta\mu_{\text{anh, Fe-NO}}$  is much larger than  $\Delta\mu_{\text{anh,Fe-CO}}$ ,  $\Delta\mu_{\text{Fe-NO}}$  should be smaller if  $\Delta\mu_{\text{bond, Fe-NO}}$  is smaller. This may explain the smaller variations in  $\bar{\nu}_{\text{Fe-NO}}$  and the lack of a strong negative correlation between  $\bar{\nu}_{\text{Fe-NO}}$  and  $\bar{\nu}_{\text{N-O}}$  in MbNO variants. We showed earlier that the Stark tuning rates for NO bound to heme ( $\Delta\mu \approx 0.12$  D/f) is about as large as that for CO ( $\Delta\mu \approx 0.12$  D/f). Therefore, the much smaller contribution of  $\Delta\mu_{\text{bond}}$  in heme–NO complexes suggests that the anharmonic contribution ( $\Delta\mu_{\text{anh}}$ ) would be dominant in  $\Delta\mu_{\text{N-O}}$  and is larger than that of C–O stretch in heme–CO complexes and that the variations in  $\bar{\nu}_{\text{N-O}}$  are mostly not from the change in its force constant. Thus, the C–O and N–O stretches in heme-bound complexes are an interesting case where the Stark tuning rates have the same overall magnitudes but different physical origins.

**Acknowledgment.** These experiments would not have been possible without the experimental and conceptual contributions by Steven Andrews, and we gratefully acknowledge his many contributions. This work was supported in part by grants from the NSF Chemistry Division and the NIH. The FTIR used for this work is located at the Stanford FEL Center supported by the Air Force Office of Scientific Research (Grant No. F49620-00-1-0349).

## References and Notes

- (1) Nakamura, H. *Q. Rev. Biophys.* **1996**, *29*, 1.
- (2) Honig, B. H.; Hubbell, W. L.; Flewelling, R. F. *Annu. Rev. Biophys. Biophys. Chem.* **1986**, *15*, 163.
- (3) Sharp, K. A.; Honig, B. *Annu. Rev. Biophys. Biophys. Chem.* **1990**, *19*, 301.
- (4) Takahashi, T.; Nakamura, H.; Wada, A. *Biopolymers* **1992**, *32*, 897.
- (5) Antosiewicz, J.; McCammon, J. A.; Gilson, M. K. *Biochemistry* **1996**, *35*, 7819.
- (6) Varadarajan, R.; Zewert, T. E.; Gray, H. B.; Boxer, S. G. *Science* **1989**, *243*, 69.
- (7) Park, K. D.; Guo, K.; Adebodun, F.; Chiu, M. L.; Sligar, S. G.; Oldfield, E. *Biochemistry* **1991**, *30*, 2333.
- (8) Steffen, M. A.; Lao, K. Q.; Boxer, S. G. *Science* **1994**, *264*, 810.
- (9) Lockhart, D. J.; Kim, P. S. *Science* **1992**, *257*, 947.
- (10) Fidy, J.; Balog, E.; Kohler, M. *Biochim. Biophys. Acta* **1998**, *1386*, 289.
- (11) Park, E. S.; Andrews, S. S.; Hu, R. B.; Boxer, S. G. *J. Phys. Chem. B* **1999**, *103*, 9813.
- (12) Chattopadhyay, A.; Boxer, S. G. *J. Am. Chem. Soc.* **1995**, *117*, 1449.
- (13) Andrews, S. S.; Boxer, S. G. *J. Phys. Chem. A* **2000**, *104*, 11853.
- (14) Park, E. S.; Thomas, M. R.; Boxer, S. G. *J. Am. Chem. Soc.* **2000**, *122*, 12297.
- (15) Hush, N. S.; Williams, M. L. *J. Mol. Spec.* **1974**, *50*, 349.
- (16) Hush, N. S.; Reimers, J. R. *J. Phys. Chem.* **1995**, *99*, 15798.
- (17) Bishop, D. M. *J. Chem. Phys.* **1993**, *98*, 3179.
- (18) Reimers, J. R.; Hush, N. S. *J. Phys. Chem. A* **1999**, *103*, 10580.
- (19) Andrews, S. S.; Boxer, S. G. *J. Phys. Chem. A* **2002**, *106*, 469.
- (20) Lambert, D. K. *J. Chem. Phys.* **1988**, *89*, 3847.
- (21) The actual field felt by the chromophore ( $F$  or sometimes denoted  $F_{\text{int}}$ ) in response to the externally applied electric field is greater than the average applied electric field ( $F_{\text{ext}}$ , the total applied voltage divided by electrode spacing in the measurements described in this paper). The difference is corrected for using the local field correction factor:  $F = fF_{\text{ext}}$ . The local field correction is in general a tensor quantity; it is treated here as a scalar and the value of  $f$  has been estimated to be between 1.1 and 1.3 (see refs 11 and 13). More details are in Böttcher, C. J. F. *Theory of Electric Polarization*; Elsevier: Amsterdam, 1973; Vol. 1. Because of uncertainty in the value of  $f$ , we report the observed values of  $|\Delta\mu|$  divided by  $f$ .
- (22) Atkins, P. W. *Physical Chemistry*, 5th ed.; W. H. Freeman and Company: New York, 1994.
- (23) Li, T. S.; Quillin, M. L.; Phillips, G. N.; Olson, J. S. *Biochemistry* **1994**, *33*, 1433.
- (24) Decatur, S. M.; Boxer, S. G. *Biochem. Biophys. Res. Comm.* **1995**, *212*, 159.
- (25) Phillips, G. N.; Teodoro, M. L.; Li, T. S.; Smith, B.; Olson, J. S. *J. Phys. Chem. B* **1999**, *103*, 8817.
- (26) Ray, G. B.; Li, X. Y.; Ibers, J. A.; Sessler, J. L.; Spiro, T. G. *J. Am. Chem. Soc.* **1994**, *116*, 162.
- (27) Andrews, S. S.; Boxer, S. G. *Rev. Sci. Instr.* **2000**, *71*, 3567.
- (28) Cys 110 on the surface of human Mb was changed to alanine to improve the yield upon purification; this mutation does not perturb ligand binding properties. See ref 29.
- (29) Varadarajan, R.; Lambright, D. G.; Boxer, S. G. *Biochemistry* **1989**, *28*, 3771.
- (30) The extinction coefficients for Hu MbCO samples were measured using the previously reported extinction coefficient of the Soret band for metaqua Hu Mb protein ( $\epsilon_{\text{Soret}} = 160$  OD/mM cm). (See ref 29.)
- (31) Antonini, E.; Brunori, M. *Hemoglobin and Myoglobin in Their Reactions With Ligands*; North-Holland Publishing Company: London, 1971.
- (32) Ormos, P.; Ansari, A.; Braunstein, D.; Cowen, B. R.; Frauenfelder, H.; Hong, M. K.; Iben, I. E. T.; Sauke, T. B.; Steinbach, P. J.; Young, R. D. *Biophys. J.* **1990**, *57*, 191.
- (33)  $\zeta$  was measured for acetone and found to be equal to 0°. Likewise  $\zeta = 0^\circ$  for an amide-containing compound, *N,N*-dimethylacetamide (data not shown). We expect that  $\zeta$  should be similar for MVK as for acetone and that NMP should be the same as *N,N*-dimethylacetamide. Therefore,  $\zeta = 0^\circ$  was used in eq 6 for the calculation of  $|\Delta\mu|$ . Generally, we expect that  $\zeta = 0^\circ$  for a localized oscillator if  $\Delta\mu_{\text{anh}}$  is dominant in the VSE because  $\Delta\mu_{\text{anh}}$  and the transition moment should be parallel. It was observed that  $\Delta\mu_{\text{anh}}$  is dominant in the VSE for acetone, MVK, and NMP (see the results).
- (34) Some of the  $\bar{\nu}_{01} - \bar{\nu}_{12}$  values were obtained in the gas phase, whereas all of the measurements in this paper were conducted in the condensed phase. The anharmonicity is expected to be similar for the condensed and the gas-phase samples if there is no direct interaction with solvents, e.g., hydrogen bonding. For acetone and MVK, the overtone bands of the CO stretch were observed at 3405 and 3337  $\text{cm}^{-1}$ , respectively, in the IR spectra under the same experimental conditions that were used in the Stark measurements; this gives 17 and 15  $\text{cm}^{-1}$ , respectively, for  $\bar{\nu}_{01} - \bar{\nu}_{12}$  (data not shown). It is difficult to assign the overtone band of the

carbonyl stretch for NMP because of a broader band and resonance mixing with other bands.

- (35) Dellepiane, G.; Overend, J. *Spectrochim. Acta* **1966**, *23*, 593.  
(36) George, W. O.; Jones, B. F.; Lewis, R.; Price, J. M. *J. Mol. Struct.* **2000**, *550*, 281.  
(37) Hamm, P.; Lim, M. H.; Hochstrasser, R. M. *J. Phys. Chem. B* **1998**, *102*, 6123.  
(38) Rector, K. D.; Kwok, A. S.; Ferrante, C.; Tokmakoff, A.; Rella, C. W.; Fayer, M. D. *J. Chem. Phys.* **1997**, *106*, 10027.  
(39) Owrutsky, J. C.; Li, M.; Locke, B.; Hochstrasser, R. M. *J. Phys. Chem.* **1995**, *99*, 4842.  
(40) Huber, K. P.; Herzberg, G. *Molecular Spectra and Molecular Structure, Vol. IV, Constants of Diatomic Molecules*; Van Nostrand Reinhold: New York, 1979.  
(41) Because CO is not very soluble in 2MeTHF and the extinction coefficient is small, the intensity of the absorption band for free CO dissolved in frozen 2MeTHF is much lower than other vibrations observed in this paper. Because of its low absorption intensity and small  $|\Delta\mu|$ , the free CO data is much noisier.  
(42) Note that the observed values of  $|\Delta\mu|$  are not corrected for the local field correction factor  $f$ . However,  $f$  is expected to be slightly larger than 1 and not to affect  $|\Delta\mu|$  significantly. See ref 21 for details.  
(43) The local field correction factor is assumed to be unity. See ref 21.

(44) Thomas, M. R.; Brown, D.; Franzen, S.; Boxer, S. G. *Biochemistry* **2001**, *40*, 15047.

(45) Tomita, T.; Hirota, S.; Ogura, T.; Olson, J. S.; Kitagawa, T. *J. Phys. Chem. B* **1999**, *103*, 7044.

(46) Here, we are assuming that the protein electric field near the Fe-CO unit is fairly uniform, so that the magnitude and the direction of the local electric fields on C-O and Fe-C (or N-O and Fe-N) are the same.

(47) Kachalova, G. S.; Popov, A. N.; Bartunik, H. D. *Science* **1999**, *284*, 473.

(48) The  $\bar{\nu}_{01} - \bar{\nu}_{12}$  value for Fe-CO stretch was reported as  $7.6 \text{ cm}^{-1}$  (Wang et al. *Proc. Natl. Acad. Sci. U.S.A.* **1995**, *92*, 9402).  $\Delta\mu_{\text{anh}}$  for the Fe-C stretch could be obtained experimentally if the IR intensity of the mode were measured; however, because of its lower stretch frequency, it is difficult to observe the Fe-CO stretch by IR.

(49) Enemark, J. H.; Feltham, R. D. *Coord. Chem. Rev.* **1974**, *13*, 339.

(50) Scheidt, W. R.; Ellison, M. K. *Acc. Chem. Res.* **1999**, *32*, 350.

(51) The maximum peak positions in the isotope difference spectra do not reflect the actual Fe-N stretch frequencies because the bandwidth of the Fe-N stretch ( $\sim 30 \text{ cm}^{-1}$ ) is larger than the isotope shift ( $\sim 14 \text{ cm}^{-1}$ ; see ref 45). Thus, the actual peak position should be obtained by simulating the isotope spectrum with two Gaussian bands, one with a positive amplitude and the other with a negative amplitude, which would each represent Fe- $^{14}\text{N}$  and Fe- $^{15}\text{N}$  stretch band, respectively.

(52) Unpublished data.